Quantitative Analysis of Axonal Transport by Using Compartmentalized and Surface Micropatterned Culture of Neurons

Hyung Joon Kim,[†,⊥] Jeong Won Park,[†] Jae Hwan Byun,[‡] Wayne W. Poon,[§] Carl W. Cotman,[§] Charless C. Fowlkes,[∥] and Noo Li Jeon*,[‡,∇]

[†]Biomedical Engineering, University of California, Irvine, California 92697, United States
[‡]School of Mechanical and Aerospace Engineering, Seoul National University, Seoul 151-744, Korea
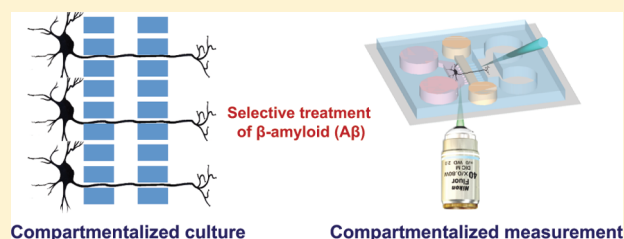[§]Institute for Memory Impairments and Neurological Disorders, University of California, Irvine, California 92697, United States
[∥]School of Information and Computer Science, University of California, Irvine, California 92697, United States

S *Supporting Information*

ABSTRACT: Mitochondria, synaptic vesicles, and other cytoplasmic constituents have to travel long distance along the axons from cell bodies to nerve terminals. Interruption of this axonal transport may contribute to many neurodegenerative diseases including Alzheimer's disease (AD). It has been recently shown that exposure of cultured neurons to β-amyloid (Aβ) resulted in severe impairment of mitochondrial transport. This Letter describes an integrated microfluidic platform that establishes surface patterned and compartmentalized culture of neurons for

Selective treatment of β-amyloid (Aβ)

Compartmentalized culture   Compartmentalized measurement

studying the effect of Aβ on mitochondria trafficking in full length of axons. We have successfully quantified the trafficking of fluorescently labeled mitochondria in distal and proximal axons using image processing. Selective treatment of Aβ in the somal or axonal compartments resulted in considerable decrease in mitochondria movement in a location dependent manner such that mitochondria trafficking slowed down more significantly proximal to the location of Aβ exposure. Furthermore, this result suggests a promising application of microfluidic technology for investigating the dysfunction of axonal transport related to neurodegenerative diseases.

KEYWORDS: β-Amyloid, axonal transport, mitochondrial trafficking, microfludics, surface micropatterning, image processing

Axonal transport has an important role in regulating physiological signal and pathological conditions in neurons. Not only do axons transmit specific signals, but they also have motor proteins-kinesin and dynein which carry cargo, internalized proteins, and organelles on the microtubules to supply the growing axon. A growing collection of experimental evidence reveals that impairment of axonal transport is associated with many neurodegenerative diseases[1−6] such as Alzheimer's disease,[7] Huntington's disease,[8] and Parkinson's disease.[9] Furthermore, recent studies showed that mitochondrial transport closely reflects the functional condition of cells[5,10] and dysfunction of transport can trigger neuronal apoptosis.[11] In Alzheimer's disease, the toxicity of β-amyloid (Aβ) and tau aggregates has been intensively studied. Yet, it is not fully understood that Aβ can trigger the impairment of mitochondrial transport as a mechanism underlying dysfunction of neural activities in neurodegenerative process.[2,12]

A natural approach to investigating these questions is to measure the morphology, locations, and movements (retrograde vs anterograde) of mitochondria in healthy neurons and compare such measurements to neurons that are in a diseased state. Tracking analysis requires single, intact neurons to be selected and the mitochondrial movement analyzed taking into account the complexity of mitochondrial dynamics including

the rapid changes in direction and fusion/fission events. However, there are several drawbacks in currently available methods to track mitochondrial movement. First, it has been performed with neurons cultured in Petri dishes such that they have randomly outgrown processes distinguishable only by morphologic characteristics.[13,14] Using a conventional Petri dish, it is difficult to identify anterograde versus retrograde transport along axons in a tangle. Second, conventional methods do not easily allow for precise spatiotemporal control of experimental conditions where one can subject axonal terminals or cell bodies for selective application of drugs or treatments.

There were interesting findings that suggest key components of an experimental platform to study mitochondrial transport in axons. Miller and Sheetz reported the first global analysis of mitochondrial transport along the full length of axons during axonal growth.[15] In addition, Tsai et al. quantified the physiological abnormalities in a transgenic model of Alzheimer's disease, which showed that the breakage of neurites occurred within and near (~15 μm of) fibrillar Aβ
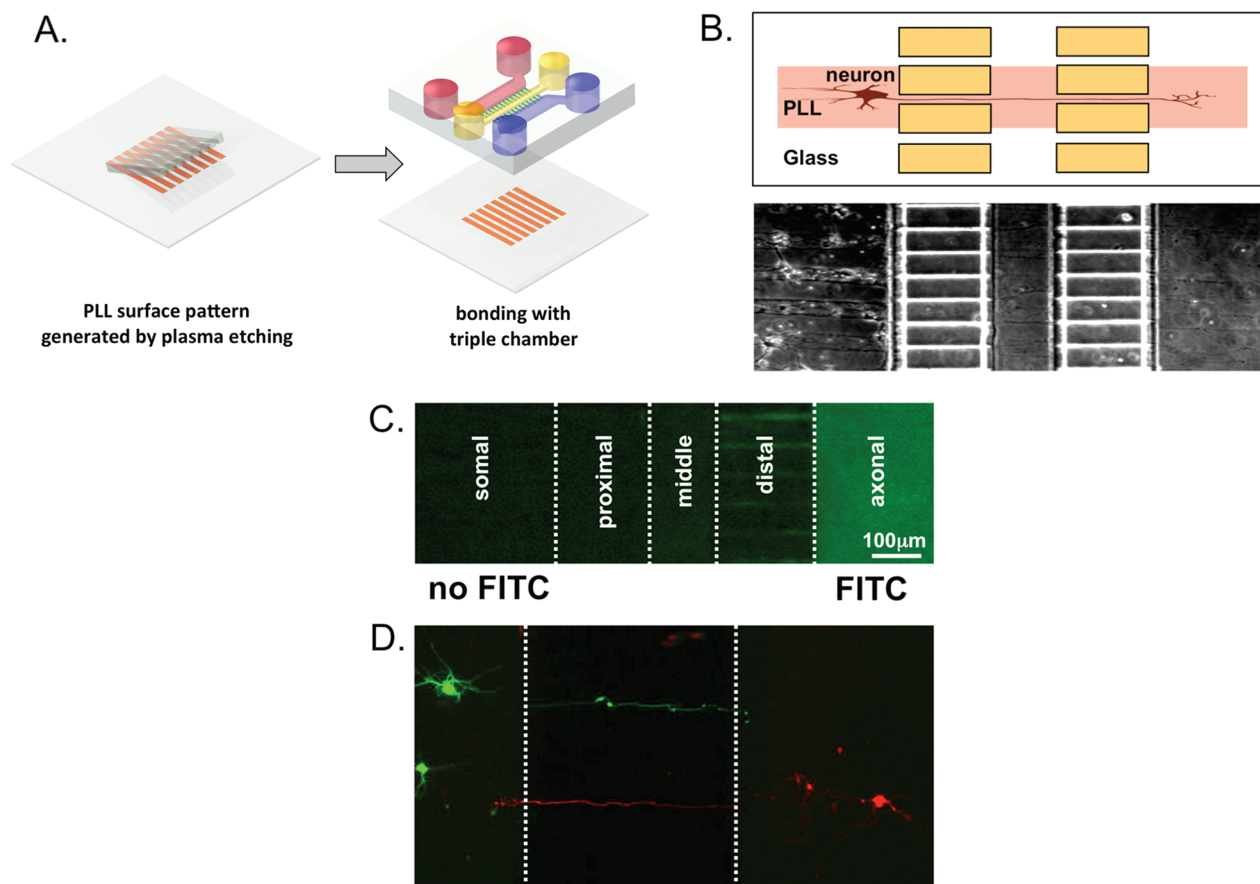
Figure 1. Schematic diagram of experimental setup. (A) Procedure for micropatterning of PLL strip on a substrate and its integration with a compartmentalized microfluidic neuron culture device. A PDMS stamp with embossed line pattern (30 × 50 μm) was placed on a PLL precoated glass coverslip. Then reactive oxygen plasma selectively removed PLL in regions that were not covered by PDMS. The substrate patterned with the PLL strip was aligned and bonded to PDMS neuron culture device. (B) Micrograph showing primary neurons cultured in the integrated microfluidic multicompartment chamber with PLL strip. Surface patterned PLL was used to control growth of axons. (C) Fluidic isolation was demonstrated by adding 10 kDa of FITC-dextran to the axonal chamber. No fluorescence was observed in the somal chamber for 24 h. (D) Neurons transfected with GFP on the left side of the device (green), and neurons transfected on the right side of the device with RFP (red). Compartmentalization and fluidic isolation allow for the transfection of two different proteins simultaneously.

deposits.[16] Previously, we reported that the microfluidic-based neuron culture platform could generate a fluidically isolated microenvironment between the soma and axonal compartment.[17,18] By utilizing this microfluidic-based neuron culture platform, we have demonstrated neuron-to-cell spread of alpha-herpes virus,[19] the involvement of local protein synthesis in axonal growth,[20] and the identification of axonal mRNA in cortical mammalian axon.[21] Recent studies have showed the use of a microfluidic device to quantify neurite outgrowth toward surface gradient[22] and to study axonal transport of NGF,[23] BDNF,[24] and tau proteins.[25] Especially in these studies for axonal transport, they solely used a microfluidic neuron culture platform such that they may bring similar difficulties in mitochondrial trafficking for regions that are not sitting in a straight microgroove region as in a random culture with a conventional Petri dish. In order to address drawbacks in previously developed methods,[23−25] we employed two methodologies: (1) integrated microfluidic device with surface micropatterning as a physical/biochemical cue for acquiring controlled axonal outgrowth and fluidic isolation and (2) automated tracking of mitochondrial movement by image processing. Through making these innovations, we developed an integrated microfluidic platform and automated image-processing for better understanding of the role of Aβ and

correlation between mitochondrial transport in axons and many neurodegenerative diseases. This platform allowed us to quantify the mitochondrial trafficking under localized exposure of Aβ at specific regions of straightly outgrowing axons.

■ RESULTS AND DISCUSSION

To apply drugs at various distances away from the somas, we secured an optimized design of a multicompartment neuron culture chamber on the poly-L-lysine (PLL) strips surface pattern based on previous studies.[26,27] Figure 1 shows a schematic view of the experimental setup including controlled axonal outgrowth and fluidic isolation property. Because of the difference (30-fold) in height between the multicompartmental channels (100 μm high) and the microgrooves (3 μm high), high fluidic resistance was achieved and one could apply drugs only at a local region of neurons, for example, proximal, distal axon, or growth cones. Also, cell bodies were plated on the PLL strip pattern and axonal outgrowth was guided along this surface pattern. We showed the fluidic isolation by adding 10 kDa of FITC-dextran at the right chamber and imaged the fluorescence signal at the opposite chamber. As shown in Figure 1C, there was no fluorescence signal at the left chamber from FITC-dextran, but at the right chamber through middle chambers even after 24 h. We finally confirmed the fluidic

434

dx.doi.org/10.1021/cn3000026 | ACS Chem. Neurosci. 2012, 3, 433−438

isolation in a microfluidic neuron culture platform by transfecting different fluorescence proteins on each compartment (Figure 1D). These results clearly show that we can apply drugs selectively at specific regions of cultured neurons and also maintain fluidic isolation for further quantitative assay. In addition, this experimental platform is suitable for studying complex and dynamic behavior of mitochondria such as anterograde versus retrograde trafficking in axons due to the confined axonal outgrowth onto the micropatterned PLL strips. Overall, we can investigate the effect of selectively applied drugs on the mitochondrial movement along multiple locations of axons.

We established an automated image-processing algorithm to quantify mitochondrial movement in axons. A mito-GFP mammalian expression vector was transfected into rat cortical neurons at DIV7. The mito-GFP localized mitochondria due to a cytochrome *c* mitochondrial localization sequence linked to the GFP. So, we could investigate the movement of mitochondrial localized GFP with time-lapse imaging. Figure 2A shows the automatic extraction of axon and a displacement-
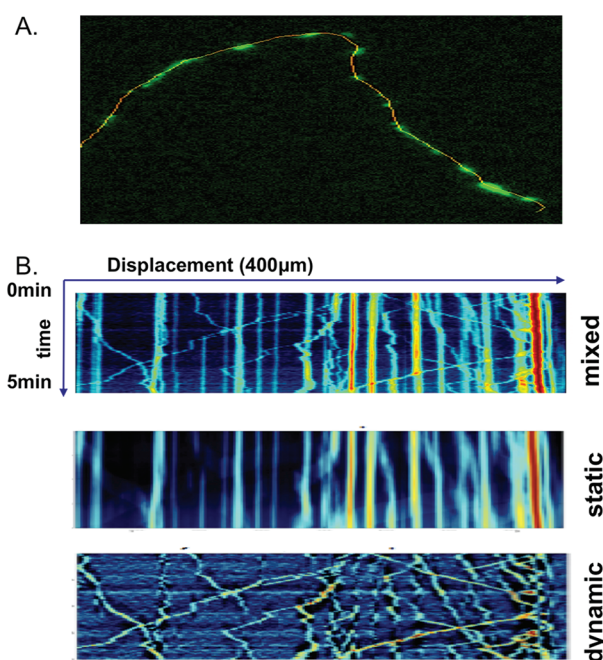

Figure 2. Demonstration of image processing. (A) mito-GFP signal along an axon (green) and extracted axon centerline (red). (B) Space−time diagram showing fluorescence along the axon centerline. Automatically decomposed into static component and dynamic component. Static and rapidly moving mitochondria are represented as vertical lines and diagonals, respectively. E-18 rat cortical neurons were cultured on nonpatterned substrate for demonstrating similar complexity in culture but not in the analysis using an automated trafficking method.

time plot showing fluorescence along the extracted axon centerline as function of time. The displacement and time of Kymograph represented the length of an axon (400 μm) and duration of time-lapse images (5 min) on the measurement, respectively. In comparison with this Kymograph, there was no significant difference in one produced by the use of painstaking hand-labeling of axons in each video frame. Also, the automated approach has generated equivalent visualizations in ∼10 s, and operating autonomously on time-lapse video data. After the identification of the axon, tracking can be formulated as a one-

dimensional problem of specifying mitochondrial locations along the axon at each time point. As shown in Figure 2B, we have decomposed the space−time data into two components, static mitochondria and dynamic mitochondria. We observed 17 nonmoving mitochondria among total 45 mitochondria in this Kymograph. In order to decompose static and dynamic entities, we extract out traces of mitochondria that have minimum displacement, 10 μm. Such decomposition will be useful in initializing tracks and counting the total number of mitochondria present.

Individual mitochondria exhibit a variety of dynamic behaviors as shown in Supporting Information Movie 1. For example, some mitochondria are largely static while others move at high speed. Mitochondria may abruptly stop and hesitate before moving on, or reverse direction entirely. It also appeared that around 40% of the neurons exhibit mitochondria that are nearly stationary, yet those neurons were still vital. Mitochondria also showed interesting interactions including apparent fusion and fission. It has been suggested that mitochondrial fission may facilitate cellular apoptosis, whereas mitochondrial fusion may protect the neuron from cellular dysfunction.[28] An appropriate algorithm for analyzing such data must take into account this range of behaviors as well as experimental artifacts, and it will automatically extract the axon location and extent based on fluorescence observed across all images in the time-lapse movie.

We analyzed the trafficking of mitochondria in multiple regions of the axon by integrating a surface patterning and multicompartmentalized microfluidic device. This type of experimental condition will provide better in vitro control to mimic the mechanism of toxic insert in brain tissue where cells are locally exposed to these toxic insults rather than being completely flooded as cells cultured on a simple Petri dish. Figure 3 shows the demonstration of mitochondrial movement
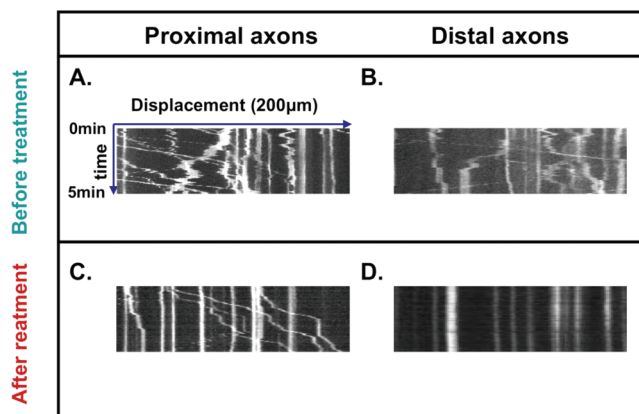

Figure 3. Trafficking of mitochondria in proximal and distal axons under selective treatment of Aβ_{1-42}. Kymographs were generated using time-lapse images that were taken before and after 1 μM of Aβ_{1-42} was applied to the axonal compartment. (A,B) Mitochondria trafficking of proximal and distal axons before treatment. (C,D) Mitochondria trafficking after 1 μM of Aβ_{1-42} treatment on axonal compartment.

at proximal and distal axons along with the localized exposure of Aβ_{1-42}. The traces of mitochondria, that is, Kymograph, were compared for before (Figure 3A and B) and after (Figure 3C and D) the treatment. As clearly shown in Figure 3D, there were almost no moving mitochondria at distal axons when we applied Aβ_{1-42} in the axonal compartment. In contrast, a

number of mitochondria on the proximal axons were maintaining their movement after the treatment (Figure 3C). To further understand these localized effects of β-amyloid, mitochondrial transport at multiple positions of axons (e.g., soma side, proximal axon, middle axon, distal axon, and axonal side) was analyzed in Figure 4. After culturing E-18 rat cortical
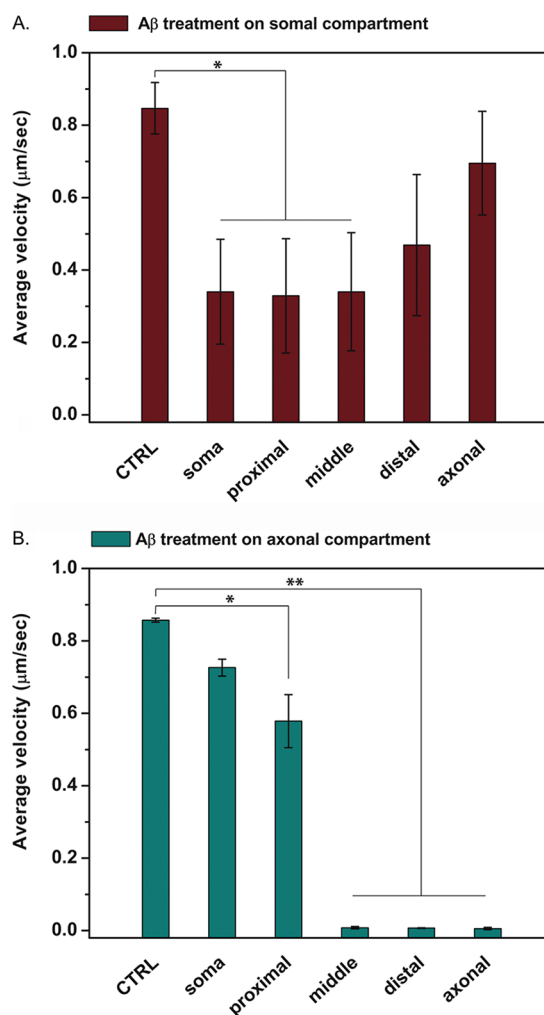

Figure 4. Quantification of mitochondrial transport at various distances away from $A\beta_{1-42}$ exposure. The average velocity of mitochondria was determined in each Kymograph for five different regions of neurons in a microfluidic device (i.e., soma side, proximal axon, middle axon, distal axon, axonal side). (A) Velocity of mitochondria following $A\beta$ treatment on soma compartment (*p = 0.0172). (B) Velocity of mitochondria following $A\beta$ treatment on axonal compartment (*p = 0.0013, **p < 0.0001). Asterisks indicate a statistical significance when comparing with the control (CTRL) at the corresponding region. Error bar indicates SEM.

neurons for 7 days in standard neuronal culture media as described in Methods, $A\beta_{1-42}$ was then added to the base medium with concentration 1 μM and applied to specified compartment followed by incubation overnight. We used synthetic $A\beta_{1-42}$ used in many studies than other types of oligomer, since $A\beta_{1-42}$ is known to have an important role in the pathogenesis of Alzheimer's disease. Recent in vivo and in vitro studies showed that soluble $A\beta$ oligomer causes decrease in the long term potentiation and the disruption of synaptic plasticity.[29,30] It has been also shown that neutrophin receptor TrkB is colocalized to mitochondrial membranes so that

neutrophins can act as signaling molecules.[31] In addition, mitochondrial movement is closely related with NGF signaling in chick dorsal root ganglia (DRG).[32] Therefore, $A\beta$ may impair synaptic function by disrupting neutrophin signaling such as BDNF[24,33] and NGF,[32] which can affect the movement of mitochondria. Our data have coincidence and extremely high statistical significance (no treatment vs treatment; p < 0.0001) with these studies that state the impairment of mitochondria movement can be caused by $A\beta$ exposure. Mitochondria stopped their movement after treating $A\beta$ on both soma and axonal compartments (Supporting Information Figure 1). We also clarified that there were no significant changes in mitochondria movement between "before treatment" and "(−) CTRL: no treatment but measured at the same timeline with treated neurons". Therefore, the control experimental set represents a healthy state of neuron. In Figure 4, localized exposure of $A\beta_{1-42}$ led to the dramatic decreases in the average velocity of mitochondria. By statistical comparison (Student's t test), axonal treatment of $A\beta_{1-42}$ resulted in higher statistical significance on velocity of mitochondria (i.e., control vs proximal axons, p = 0.0013; control vs distal axons, p < 0.0001) than in the case of somal treatment (i.e., control vs proximal axons, p = 0.0172; control vs distal axons, p = 0.1062, statistically significant for soma, proximal, and middle axons but not for distal axons). Our findings show that the effect of $A\beta$ on mitochondria transport can be described as "localized", which implies fluidically isolated application of $A\beta$ in the somal or axonal compartments resulted in a remarkable decrease in mitochondria movement more significantly in the vicinity of $A\beta$ exposure. The soluble $A\beta_{1-42}$ is known to undergo a slow aggregation such that it changes from monomer to fibrilis.[34] Importantly, we enabled to expose $A\beta_{1-42}$ on cell bodies or axons alone by using a fluidically isolated microenvironment, replicating anatomical features in the brain. While $A\beta_{1-42}$ diffuses through microgrooves, that is, from axonal compartment to proximal axonal region, slow aggregation can be preceded at a closer location of exposure. Our observation also has coincidence with the previous study[12] that concluded aged $A\beta_{1-42}$ (consisting more fibirils) appeared to be more potent to impairment of mitochondria transport than a freshly prepared one (consisting of monomers). To further examine this phenomenon, we could design an advanced imaging system that can track both mitochondria transport and the formation of fibril $A\beta$. Overall, we may conclude that fluidically isolated application of $A\beta$ on the somal or axonal compartments resulted in considerable decrease in mitochondria movement in a location dependent manner.

In this Letter, we described an experimental platform to accurately record and quantitatively investigate the movements of mitochondria along the axon under precisely controlled microenvironment. This entailed (1) control of the outgrowth of neurons by combining surface micropatterning and multi-compartmentalized microfluidic neuron culture platform for monitoring mitochondrial trafficking along the full length of the axon, (2) development of automated localization and tracking of mitochondrial movement in time-lapse sequences, and (3) analysis of the effect of selectively applied $A\beta$ on the mitochondrial movement at various regions of the axon. Investigating mitochondrial trafficking in neurons can be served as an important tool to understand cellular transport behavior in healthy axons and form a basis for comparing with neurons subject to axonal transport dysfunction observed in many neurodegenerative diseases. An integrated microfluidic platform

in this study not only is critical to form a basic understanding of axonal transport but also paves the way to large scale experiments such as screening large drug libraries where manual analysis of subtle effects is entirely infeasible.

METHODS

Preparation of Microfluidic Culture Devices. The PDMS (Sylgard 184, Dow Corning, MI) chambers were made using soft lithography and replica molding as described previously.[17,18] Briefly, photolithography was used to make two layers of negative photoresist on a silicon wafer, resulting in a master with positive relief patterns of cell culture compartments (1.5 mm wide, 7 mm long, 100 μm high) and microgrooves (7.5 μm wide, 3 μm high). A PDMS–prepolymer mixture was poured over the positive relief master to obtain a negative replica-molded piece. After curing, the PDMS was peeled away from the master. The reservoirs were punched with a sharpened needle and then sterilized by autoclaving.

Preparation of PLL Patterned Glass Coverslip and Its Integration with Microfluidic Devices. A detailed schematic procedure is shown in Figure 1A. The glass coverslip was coated with 0.5 mg/mL poly-L-lysine (PLL, MW 70 000–150 000, Sigma, St. Louis, MO) for overnight. They were washed twice with sterilized water for 30 min to remove remaining poly-L-lysine. A PDMS stamp having the desired surface embossed pattern was fabricated by the same process as PDMS culture devices and placed on the PLL precoated glass coverslip. It was exposed to reactive oxygen plasma (30 W, 200–600 mTorr, Harrick Scientific, Pleasantville, NY) for 10 s to create a PLL stripe micropattern on the substrate. The sterilized PDMS devices were aligned and assembled with the PLL stripe micropattern on the glass coverslips immediately after oxygen plasma treatment to form an irreversible seal.[18,27,35]

Cortical Neurons Preparation. In accordance with AAALAC guidelines, rodents were housed in the vivarium of the Gillespie Neuroscience Research Laboratories at the University of California, Irvine. We prepared cortical dissociated neurons from embryonic rat (E18) as described previously. Briefly, cortexes of E18 rat embryos were dissected and resuspended in a trypsin solution (0.125% trypsin in CMF-HBSS containing 0.5 mM EDTA) for 7 min at 37 °C or 25 min at ambient temperature. Trypsinization was stopped with Dulbecco's modified Eagle's medium (DMEM) containing 10% fetal bovine serum (FBS), the tissue was centrifuged at 1000 rpm for 1 min, and the resulting cell pellet was resuspended in 2 mL of culture medium (neurobasal medium, Gibco 21103, containing B27 supplement, Gibco 17504, GlutaMAX, Gibco 35050, and penicillin-streptomycin, Gibco 15070). Cells were plated at densities of 3–5 × 10^6 cells/mL in microfluidic devices.

Plasmids and Proteins. Vectors were purchased, subcloned in house, or received as kind gifts from other researchers. The pEGFP-N1 vector was purchased from Clontech (Mountain View, CA). The roGFP-mito that is a modified version of pEYFP-mito (Clontech, Mountain View, CA) was kindly provided by Dr. Lin from the Howard Hughes Medical Institute (San Diego, CA). The RFP gene contained in the pDsRed1 vector (Clontech, Mountain View, CA) was subcloned into a mammalian expression vector pcDNA3.1+ (Invitrogen, Carlsbad, CA).

Fluorescent Labeling of Mitochondria. Neurons were transfected after 7 days of culture. For one device, 0.8 μg of the appropriate vector was mixed with 50 μL of OptiMEM (Invitrogen, Carlsbad, CA) and incubated at room temperature (RT) for 5 min. In a separate tube, 50 μL of OptMEM was mixed with 2 μL of lipofectamine 2000 (L2K) (Invitrogen, Carlsbad, CA) and incubated at RT for 5 min. After the 5 min incubation of each individual tube, the DNA/OptiMEM and L2K/OptiMEM were mixed and incubated for an additional 20 min at RT. The mixture of DNA/L2K/OptiMEM was added to the soma side of the device. After adding the transfection mixture, the neurons were incubated at 37 °C, 5% CO_2 for 3 h. After that, the tranfection mixture was removed and fresh media was added twice for washing. And then the neurons were incubated for at least 48 h before imaging.

Preparation of Aβ Oligomer. Lyophilized Aβ oligomer as a HFIP film (Chemicon, Temecula, CA) was stored at −80 °C until used. Aβ was dissolved in neat, sterile dimethyl sulfoxide (DMSO; 5 mM) and diluted in phosphate buffered saline (PBS), pH 7.4 to 100 mM and aged overnight (4 °C), centrifuged (14 000g, 10 min, 4 °C), and the supernatants transferred to fresh Eppendorf tubes and stored at 4 °C until use.

Quantifying Mitochondrial Movement Using Image Processing. Fluorescently labeled mitochondria were imaged 48 h after transfection. A Nikon TE 200 Eclipse (Nikon, Melville, NY) microscope equipped with a CoolSnap CCD camera (Photometrics, Tucson, AZ) was used to take time-lapse images. Images were taken at the same axon/location before and after Aβ treatment in every 3 s during 5 min. In order to track the movement of mitochondria by hand, we used the z-projection function and multiple Kymograph plug-in of ImageJ (National Institutes of Health, Bethesda, MD). For automatic trafficking of mitochondria, a MATLAB algorithm was coded to extract axon segment centerlines from the time-lapse movie. Then, it performed initial one-dimensional tracking and generated Kymographs. A MATLAB algorithm was validated by comparing the result using ImageJ and automatically generated data. Kymographs were generated for each axon, and the average velocity of mitochondria was evaluated from each track. Quantification was performed for at least three axons per movie, and each axon (in field of view) has about 10–15 mitochondria such that the average velocity was determined for 30–45 mitochondria, and a statistical comparison of control (before treatment, i.e., same set of neurons in healthy state) versus Aβ treated neurons.

ASSOCIATED CONTENT

Ⓢ Supporting Information

Figure 1: Quantitative measurement of mitochondria transport on the control experiment. Asterisks indicate a statistical significance when comparing "before treatment" and the negative control with positive control (both side treatment). Error bar indicates SEM. Movie 1: Live cell imaging shows fluorescence labeled mitochondria in the microgrooves of microfluidics device. Mitochondria trafficking on three axons in this field of view could be evaluated. This material is available free of charge via the Internet at http://pubs.acs.org.

AUTHOR INFORMATION

Corresponding Author
*Telephone 1-82-2-880-7111. Fax: 1-82-2-880-7119. E-mail: njeon@snu.ac.kr.

Present Addresses
[⊥]Laboratory of Genetics, The Salk Institute for Biological Studies, 10010 North Torrey Pines Road, La Jolla, California 92037, United States.
[∇]WCU Multiscale Mechanical Design, School of Mechanical and Aerospace Engineering, Seoul National University, Seoul 151-744, Korea.

Author Contributions
H.J.K. contributed to experimental design, performed research, analyzed data, and contributed to writing of the manuscript. J.W.P., J.H.B., and W.W.P. contributed to experimental design and manuscript preparation. C.C.F. contributed to data analysis using MATLAB. C.W.C. and N.L.J. provided research oversight, technical direction, and manuscript preparation.

437

dx.doi.org/10.1021/cn3000026 | ACS Chem. Neurosci. 2012, 3, 433–438

Notes

The authors declare no competing financial interest.

■ REFERENCES

(1) Chevalier-Larsen, E., and Holzbaur, E. L. (2006) Axonal transport and neurodegenerative disease. *Biochim. Biophys. Acta 1762*, 1094–1108.

(2) Morfini, G. A., Burns, M., Binder, L. I., Kanaan, N. M., LaPointe, N., Bosco, D. A., Brown, R. H. Jr., Brown, H., Tiwari, A., Hayward, L., Edgar, J., Nave, K. A., Garberrn, J., Atagi, Y., Song, Y., Pigino, G., and Brady, S. T. (2009) Axonal transport defects in neurodegenerative diseases. *J. Neurosci. 29*, 12776–12786.

(3) Chang, D. T., Honick, A. S., and Reynolds, I. J. (2006) Mitochondrial trafficking to synapses in cultured primary cortical neurons. *J. Neurosci. 26*, 7035–7045.

(4) Ebneth, A., Godemann, R., Stamer, K., Illenberger, S., Trinczek, B., and Mandelkow, E. (1998) Overexpression of tau protein inhibits kinesin-dependent trafficking of vesicles, mitochondria, and endoplasmic reticulum: implications for Alzheimer's disease. *J. Cell Biol. 143*, 777–794.

(5) Malaiyandi, L. M., Honick, A. S., Rintoul, G. L., Wang, Q. J., and Reynolds, I. J. (2005) Zn^{2+} inhibits mitochondrial movement in neurons by phosphatidylinositol 3-kinase activation. *J. Neurosci. 25*, 9507–9514.

(6) Szeto, H. H. (2006) Mitochondria-targeted peptide antioxidants: novel neuroprotective agents. *AAPS J. 8*, E521–531.

(7) Lustbader, J. W., Cirilli, M., Lin, C., Xu, H. W., Takuma, K., Wang, N., Caspersen, C., Chen, X., Pollak, S., Chaney, M., Trinchese, F., Liu, S., Gunn-Moore, F., Lue, L. F., Walker, D. G., Kuppusamy, P., Zewier, Z. L., Arancio, O., Stern, D., Yan, S. S., and Wu, H. (2004) ABAD directly links Aβ to mitochondrial toxicity in Alzheimer's disease. *Science 304*, 448–452.

(8) Bae, B. I., Xu, H., Igarashi, S., Fujimuro, M., Agrawal, N., Taya, Y., Hayward, S. D., Moran, T. H., Montell, C., Ross, C. A., Snyder, S. H., and Sawa, A. (2005) p53 mediates cellular dysfunction and behavioral abnormalities in Huntington's disease. *Neuron 47*, 29–41.

(9) Valente, E. M., Abou-Sleiman, P. M., Caputo, V., Muqit, M. M., Harvey, K., Gispert, S., Ali, Z., Del Turco, D., Bentivoglio, A. R., Healy, D. G., Albanese, A., Nussbaum, R., Gonzalez-Maldonado, R., Deller, T., Salvi, S., Cortelli, P., Gilks, W. P., Latchman, D. S., Harvey, R. J., Dallapiccola, B., Auburger, G., and Wood, N. W. (2004) Hereditary early-onset Parkinson's disease caused by mutations in PINK1. *Science 304*, 1158–1160.

(10) Hollenbeck, P. J., and Saxton, W. M. (2005) The axonal transport of mitochondria. *J. Cell Sci. 118*, 5411–5419.

(11) Wallace, D. C. (2001) Mitochondrial defects in neurodegenerative disease. *Ment. Retard. Dev. Disability Res. Rev. 7*, 158–166.

(12) Rui, Y., Tiwari, P., Xie, Z., and Zheng, J. Q. (2006) Acute impairment of mitochondrial trafficking by beta-amyloid peptides in hippocampal neurons. *J. Neurosci. 26*, 10480–10487.

(13) Hollenbeck, P. J. (1996) The pattern and mechanism of mitochondrial transport in axons. *Front. Biosci. 1*, d91–102.

(14) Ligon, L. A., and Steward, O. (2000) Role of microtubules and actin filaments in the movement of mitochondria in the axons and dendrites of cultured hippocampal neurons. *J. Comp. Neurol. 427*, 351–361.

(15) Miller, K. E., and Sheetz, M. P. (2006) Direct evidence for coherent low velocity axonal transport of mitochondria. *J. Cell Biol. 173*, 373–381.

(16) Tsai, J., Grutzendler, J., Duff, K., and Gan, W. B. (2004) Fibrillar amyloid deposition leads to local synaptic abnormalities and breakage of neuronal branches. *Nat. Neurosci. 7*, 1181–1183.

(17) Taylor, A. M., Blurton-Jones, M., Rhee, S. W., Cribbs, D. H., Cotman, C. W., and Jeon, N. L. (2005) A microfluidic culture platform for CNS axonal injury, regeneration and transport. *Nat. Methods 2*, 599–605.

(18) Park, J. W., Vahidi, B., Taylor, A. M., Rhee, S. W., and Jeon, N. L. (2006) Microfluidic culture platform for neuroscience research. *Nat. Protoc. 1*, 2128–2136.

(19) Liu, W. W., Goodhouse, J., Jeon, N. L., and Enquist, L. W. (2008) A microfluidic chamber for analysis of neuron-to-cell spread and axonal transport of an alpha-herpesvirus. *PLoS ONE 3*, e2382.

(20) Hengst, U., Deglincerti, A., Kim, H. J., Jeon, N. L., and Jaffrey, S. R. (2009) Axonal elongation triggered by stimulus-induced local translation of a polarity complex protein. *Nat. Cell Biol. 11*, 1024–1030.

(21) Taylor, A. M., Berchtold, N. C., Perreau, V. M., Tu, C. H., Jeon, N. L., and Cotman, C. W. (2009) Axonal mRNA in uninjured and regenerating cortical mammalian axons. *J. Neurosci. 29*, 4697–4707.

(22) Millet, L. J., Stewart, M. E., Nuzzo, R. G., and Gillette, M. U. (2010) Guiding neuron development with planar surface gradients of substrate cues deposited using microfluidic devices. *Lab Chip 10*, 1525–1535.

(23) Zhang, K., Osakada, Y., Vrljic, M., Chen, L., Mudrakola, H. V., and Cui, B. (2010) Single-molecule imaging of NGF axonal transport in microfluidic devices. *Lab Chip 10*, 2566–2573.

(24) Poon, W. W., Blurton-Jones, M., Tu, C. H., Feinberg, L. M., Chabrier, M. A., Harris, J. W., Jeon, N. L., and Cotman, C. W. (2011) beta-Amyloid impairs axonal BDNF retrograde trafficking. *Neurobiol. Aging 32*, 821–833.

(25) Stoothoff, W., Jones, P. B., Spires-Jones, T. L., Joyner, D., Chhabra, E., Bercury, K., Fan, Z., Xie, H., Bacskai, B., Edd, J., Irimia, D., and Hyman, B. T. (2009) Differential effect of three-repeat and four-repeat tau on mitochondrial axonal transport. *J. Neurochem. 111*, 417–427.

(26) Rhee, S. W., Taylor, A. M., Cribbs, D. H., Cotman, C. W., and Jeon, N. L. (2007) External force-assisted cell positioning inside microfluidic devices. *Biomed. Microdevices 9*, 15–23.

(27) Rhee, S. W., Taylor, A. M., Tu, C. H., Cribbs, D. H., Cotman, C. W., and Jeon, N. L. (2005) Patterned cell culture inside microfluidic devices. *Lab Chip 5*, 102–107.

(28) Chen, H., and Chan, D. C. (2005) Emerging functions of mammalian mitochondrial fusion and fission. *Hum. Mol. Genet. 14*, R283–289.

(29) Billings, L. M., Oddo, S., Green, K. N., McGaugh, J. L., and LaFerla, F. M. (2005) Intraneuronal Abeta causes the onset of early Alzheimer's disease-related cognitive deficits in transgenic mice. *Neuron 45*, 675–688.

(30) Cleary, J. P., Walsh, D. M., Hofmeister, J. J., Shankar, G. M., Kuskowski, M. A., Selkoe, D. J., and Ashe, K. H. (2005) Natural oligomers of the amyloid-beta protein specifically disrupt cognitive function. *Nat. Neurosci 8*, 79–84.

(31) Wiedemann, F. R., Siemen, D., Mawrin, C., Horn, T. F., and Dietzmann, K. (2006) The neurotrophin receptor TrkB is colocalized to mitochondrial membranes. *Int. J. Biochem. Cell Biol. 38*, 610–620.

(32) Chada, S. R., and Hollenbeck, P. J. (2003) Mitochondrial movement and positioning in axons: the role of growth factor signaling. *J. Exp. Biol. 206*, 1985–1992.

(33) Tong, L., Balazs, R., Thornton, P. L., and Cotman, C. W. (2004) Beta-amyloid peptide at sublethal concentrations downregulates brain-derived neurotrophic factor functions in cultured cortical neurons. *J. Neurosci. 24*, 6799–6809.

(34) Parbhu, A., Lin, H., Thimm, J., and Lal, R. (2002) Imaging real-time aggregation of amyloid beta protein (1–42) by atomic force microscopy. *Peptides 23*, 1265–1270.

(35) Duffy, D. C., McDonald, J. C., Schueller, O. J. A., and Whitesides, G. M. (1998) Rapid prototyping of microfluidic systems in poly(dimethylsiloxane). *Anal. Chem. 70*, 4974–4984.